

Identifying attractors in a boost converter

IVAN FLEGAR, DENIS PELIN, TOMISLAV ADAMOVIĆ

Faculty of Electrical Engineering

University of Osijek

Kneza Trpimira 2b, 31000 Osijek

CROATIA

pelin@etfos.hr, URL: <http://www.etfos.hr>

Abstract: – A boost converter controlled by naturally-sampled constant frequency pulse-width modulation in discontinuous conduction mode of operation is analysed. By varying the input voltage only limit cycles and strange attractors are identified by computer simulation as well as by experiments on the physical model of the boost converter. A good agreement between simulation results and experiments is obtained.

Key-words: - boost converter , limit cycles, strange attractors, Poincaré maps, bifurcation diagram.

1 Introduction

One of the most active research topics in power electronics is the analysis of all possible modes of operation of the boost converter. It is motivated by the widespread application of this type of dc converters as a basic building block of single-phase power factor correction circuits.

The correct design of the boost converter assumes that all possible modes of operation and their dependences on variation of converter parameters are known in advance. In this way it is possible to avoid certain undesirable performance during service such as occurrence of increased dc output ripple or audible sound.

The boost converter is an example of a time-varying nonlinear dynamical system exhibiting a great variety of modes of operation, some of them of a truly complex nature. The modes of operation of the boost converter are strongly related to their long-term behaviour, that is, to the structure of its attractors. By an attractor we mean a set of points to which the state vector representing the dynamical system returns after a perturbation. Two types of attractors have been observed in boost converter practice: limit cycles that correspond to periodic oscillations and strange attractors that correspond to chaos [1-5].

To study the modes of operation of the boost converter computer simulation and real experiments have been used and presented in this paper. The tools of the qualitative theory of dynamical systems such as Poincaré maps and bifurcation diagrams have been also used. For a fixed set of converter parameters and varying the input voltage only, the modes of operation predicted by computer simulation are compared with the modes of operation obtained by measurements.

2 State equations

The functional diagram of the boost converter is shown in Fig. 1. The discontinuous conduction mode of operation is assumed. Thus the boost converter can be thought of as a piece-wise linear time-varying system subjected to three changes of power circuit topology in a period of operation T .

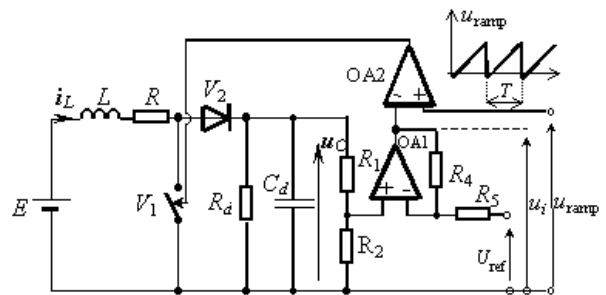


Fig.1 Functional diagram of the boost converter

- a) When $u_{\text{ramp}} \geq u_i$, the controlled switch V_1 is in the ON-state and the diode V_2 is in the OFF-state. The state equations are:

$$\frac{du_c}{dt} = \frac{1}{CR_d} u_c \quad (1)$$

$$\frac{di_L}{dt} = \frac{1}{L} (E - Ri_L)$$

where the capacitor voltage u_c and inductor current i_L are state variables.

- b) When $u_{\text{ramp}} < u_i$, $i_L > 0$, the controlled switch V_1 is in the OFF-state and the diode V_2 is in the ON-state. The state equations are:

$$\frac{du_c}{dt} = \frac{1}{C} \left(i_L - \frac{u_c}{R_d} \right) \quad (2)$$

$$\frac{di_L}{dt} = \frac{1}{L} (E - Ri_L - u_c)$$

- c) When $u_{ramp} < u_i$, $i_L=0$, the controlled switch V_1 and the diode V_2 are in the OFF-state. The state equations are:

$$\frac{du_C}{dt} = \frac{1}{CR_d} u_C \quad (3)$$

$$i_L = 0$$

According to Fig.1 the input voltage of the operational amplifier OA2 $u_i(t)$ is given by

$$u_i = \frac{-R_4}{R_5} U_{ref} + \left(1 + \frac{R_4}{R_5}\right) \cdot \frac{R_2}{R_1 + R_2} u_C \quad (4)$$

The ramp voltage

$$u_{ramp} = \frac{3}{T} t + 0,7 \text{ [V]} \quad (5)$$

is obtained by measurements carried out on the constant frequency pulse-width modulator MC34060 which was used in the physical model of the boost converter.

3 Simulation results

All simulations were carried out for a fixed set of converter parameters: $R_1=22k\Omega$, $R_2=1.22k\Omega$, $R_4=2.7M\Omega$, $R_5=3.9k\Omega$, $R=0.73\Omega$, $L=698 \mu\text{H}$, $C=470\mu\text{F}$, $R_d=56\Omega$, $U_{ref}=5\text{V}$ and $T=500\mu\text{s}$ with the dc input voltage E varying only. The fourth-order Runge-Kutta method of numerical integration with the fixed step size of integration $h=50 \text{ ns}$ was used.

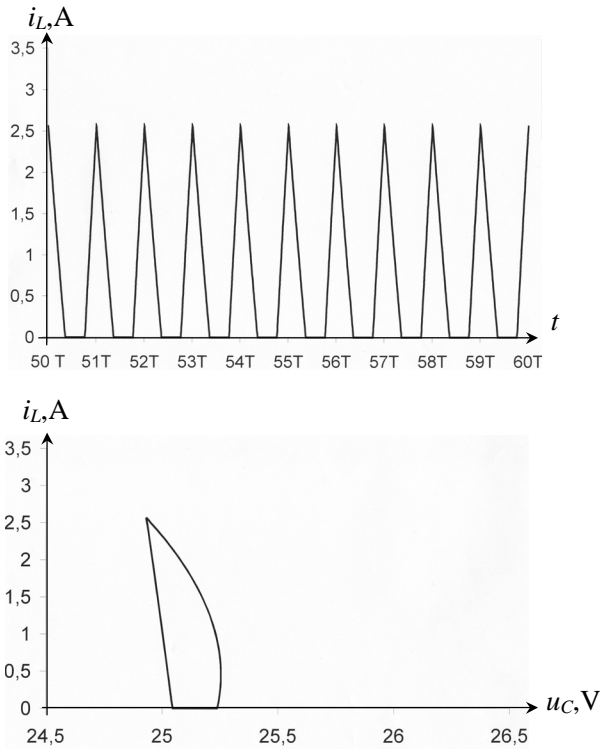


Fig.2 a) Calculated inductor current at $E=16\text{V}$
b) Calculated trajectory in the phase plane u_C-i_L characterising period-on operation

Simulation results are presented as steady-state waveforms of the state variables or as trajectories in the phase plane u_C-i_L . Fig.2 shows the fundamental period operation (period one operation) at $E=16 \text{ V}$ and Fig.3 shows the chaotic operation at $E=21 \text{ V}$ displaying waveforms of inductor current i_L as well as trajectories in the phase plane u_C-i_L .

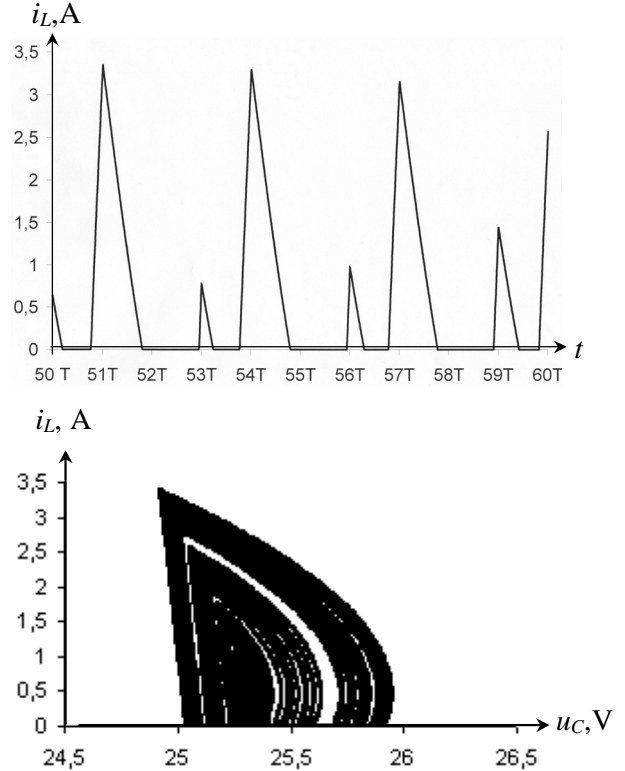


Fig.3 a) Calculated inductor current at $E=21\text{V}$
b) Calculated trajectory in the phase plane u_C-i_L characterising chaotic operation

3.1 Poincaré maps

The strange attractors associated with chaos may be displayed on Poincaré maps. For a nonautonomous dynamical system, as it is in our case, a pair of state variables u_C and i_L is chosen. Instead of plotting the complete trajectory in the phase plane, the state variables are sampled, once per drive cycle. Here, the 1000 samples of inductor current $i_L(t_k)$ and capacitor voltage $u_C(t_k)$ are taken at the intervals

$$t_k = t_0 + kT, \quad k = 50, 51, \dots, 1049 \quad (6)$$

where t_0 is an instant chosen at will. Each sample is plotted as a point in the phase plane. Though the boost converter is at steady state after few periods, the safety margin of 50 periods was accepted. In this way we are sure that period- N operation of the converter will be represented by exactly N points in the phase plane. In chaotic mode of operation, as it is seen in Fig.4, the sample points form a characteristic figure revealing the underlying structure of the strange attractor.

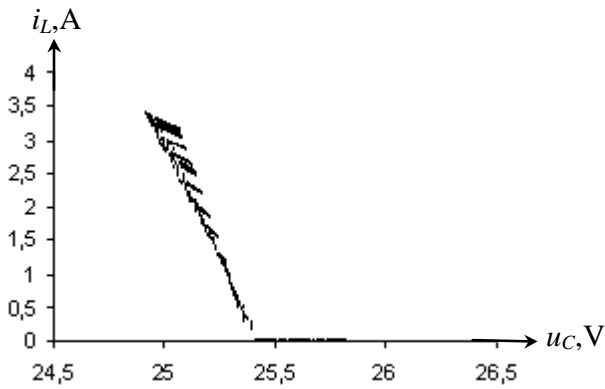


Fig.4 Poincaré map of the strange attractor characterising chaotic operation at $E=21V, (t_0=0)$.

Chaos is a real world phenomenon. Therefore, we believe that qualitative properties of the attractor, represented by the corresponding Poincaré map, ought to remain invariant with regard to different mathematical descriptions of the considered dynamical system as well as to the different initial conditions or different computer precisions used by numerical integration of state equations.

On the other hand, it is well known that the time evolution of state variables in chaotic operation strongly depends on initial conditions. Thus if we start the numerical integration of state equations from the two sufficiently close sets of initial conditions, the solutions remain bounded but diverge each from the other. The same applies to the case when numerical integration of state equations is carried out with different computer precisions. Nevertheless, in any case the corresponding Poincaré maps preserve the characteristic figure, displaying the robustness of chaotic phenomena.

To illustrate this five consecutive points (150,151,152,153,154) on the Poincaré maps at $E=21V$ for two different computer precisions are shown in Fig.5. In the first case a software tool was

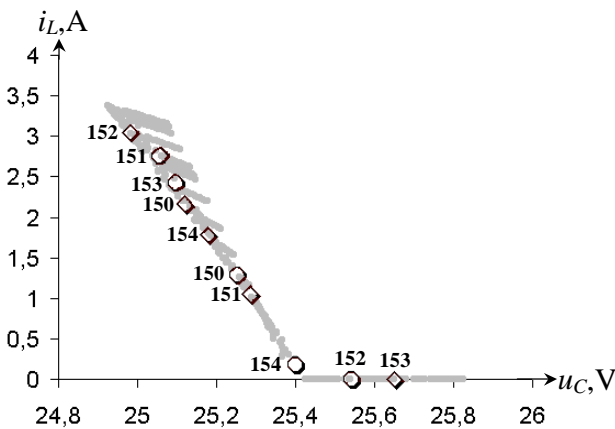


Fig.5 Five consecutive points on the Poincaré map at $E=21V$ obtained with two different computer precisions
 \diamond (64 bit word), \circ (32 bit word)

used in which a real number was represented by the 32 bit word and in the second case a real number was represented by the 64 bit word. The corresponding points do not coincide, but nevertheless they lie on the same characteristic figure.

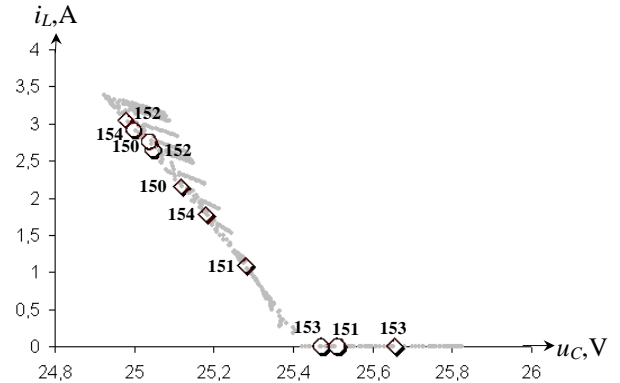


Fig.6 Five consecutive points on the Poincaré map at $E=21V$ obtained with two different initial conditions

\diamond (25V,0A), \circ (25,001V,0A)

The same applies to the case where sample points $[u_C(t_k), i_L(t_k)]$ are obtained by numerical integration of state equations with the same computer precisions and starting with two sets of initial conditions $[25V;0A]$ and $[25.001V;0A]$ respectively as it is shown in Fig.6.

The characteristic figure representing the strange attractor is preserved also by varying the sampling instant t_0 . by increasing t_0 the characteristic figures remain qualitatively similar and rotate clockwise in the phase plane, Fig.7.

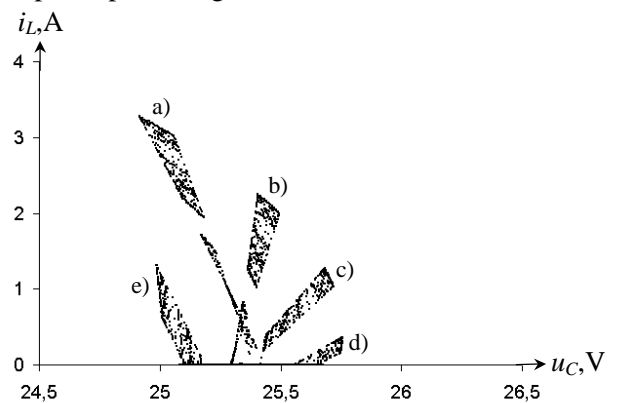


Fig.7 Poincaré maps at $E=21V$ with different instants of sampling t_0 : a) $t_0=0$, b) $t_0=T/5$, c) $t_0=2T/5$, d) $t_0=3T/5$, e) $t_0=4T/5$.

3.2 Bifurcation diagram

The most complete insight into the transition between different modes of operation provides the bifurcation diagram. Instead of two state variables, a single state variable is selected for display. The other axis of the diagram is used to sweep a selected system parameter. Here, the bifurcation diagram is generated by using the same values of inductor

current $i_L(t_k)$ as those used to generate Poincaré maps. In the same way as before the period- N operation of the converter will be represented by exactly N points on the bifurcation diagram for a particular value of input voltage E which was selected as a variable system parameter. Also, the random dispersion of points of sampled variable i_L indicates the chaotic operation. Fig.8 shows the bifurcation diagram as the input voltage E is varied from 15V to 24V. Period-doubling route to chaos, chaotic regions as well as period-three operation are easily recognised.

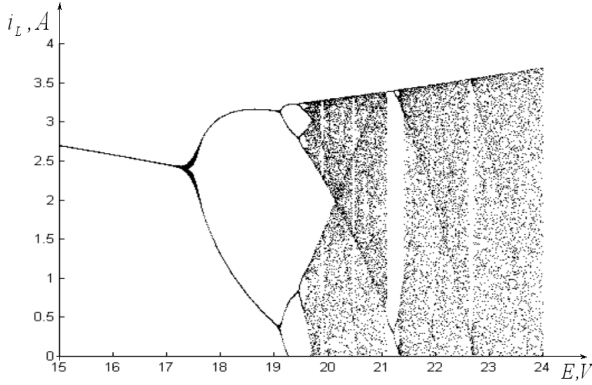


Fig.8 Bifurcation diagram

4 Experiments

A physical model of the boost converter was built. To identify all possible modes of operation

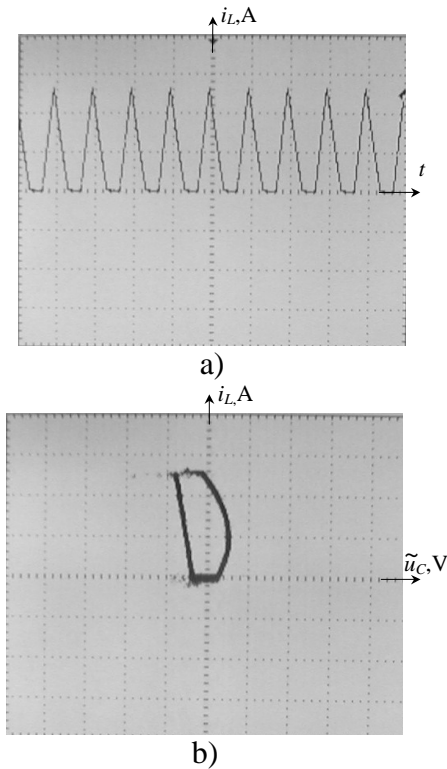


Fig.9 a) Measured inductor current at $E=16V$ (1A/div, 500 μ s/div)
b) Measured trajectory in the phase plane (300mV/div, 1A/div)

experimentally we observed at particular values of the input voltage E the trajectories in the phase plane $\tilde{u}_C - i_L$, where \tilde{u}_C is the ac component of the capacitor voltage. Three trajectories characterising period-one operation, period-two operation and chaos are shown in Fig.9, Fig.10 and Fig.11 respectively.

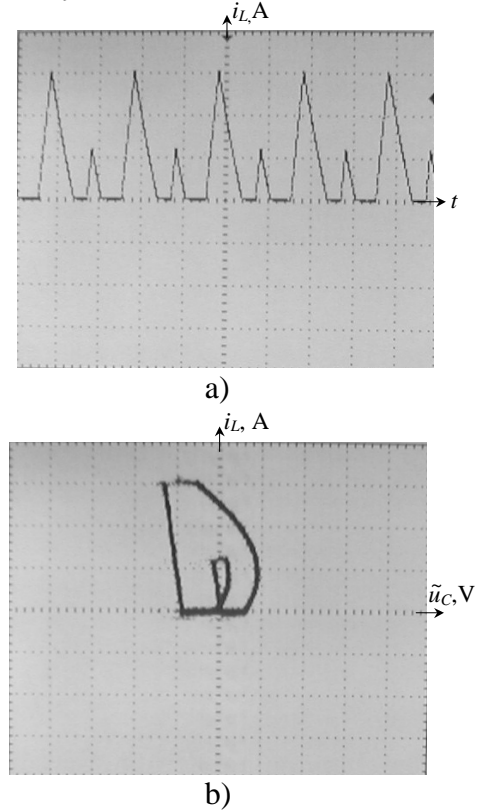


Fig.10 a) Measured inductor current at $E=18V$ (1A/div, 500 μ s/div)
b) Measured trajectory in the phase plane (300mV/div, 1A/div)

Results of measurements and results obtained from the computed bifurcation diagram $[E, i_L(t_k)]$, agree very well as it is shown in Table 1.

Modes of operation	E, V	
	Measured values	Computed values
Period-one operation	12-17.5	12-17
Period-two operation	17.5-19.1	17-19.2
Period-four operation	19.1-19.3	19.2-19.3
Period-eight operation	/	19.3-19.4
Chaos	19.3-21.2	19.4-21.1
Period-three operation	21.2-21.4	21.1-21.3

Table 1. Modes of operation of the boost converter

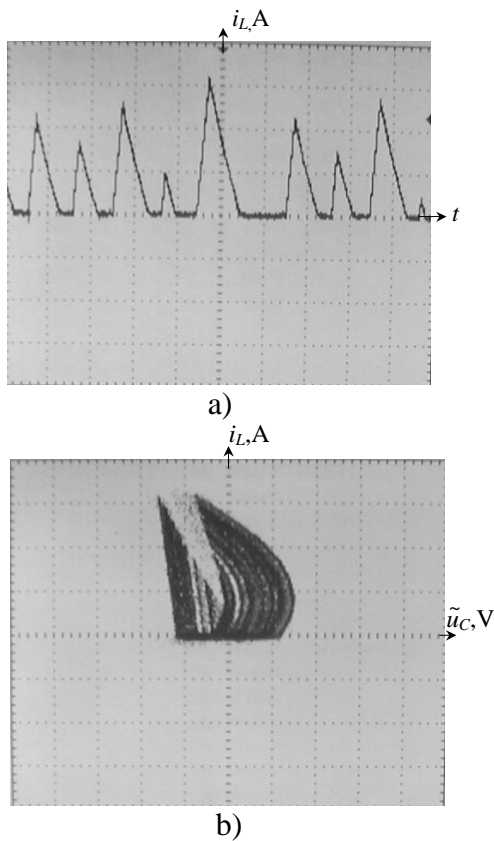


Fig.11 a) Measured inductor current at $E=21V$
 (1A/div, 500 μ s/div)
 b) Measured trajectory in the phase plane
 (300mV/div, 1A/div)

5 Conclusions

The long-term behaviour of the analysed boost converter is characterised by two types of attractors: limit cycles and strange attractors. For a fixed set of converter parameters and varying the input voltage

only the limit cycles characterising period-doubling process are obtained. Invariance of the characteristic figure on Poincaré map representing the strange attractor at a particular value of the input voltage indicates the robustness of chaotic phenomena.

A close accordance between bifurcation points obtained from the computed bifurcation diagram $[E, i_L(t_k)]$ and measured bifurcation points implies the validity of the chosen mathematical model of the boost converter. It can be used to predict all possible modes of operation occurring actually in applications.

References:

- [1] J.H.B.Deane, "Chaos in current-mode controlled boost DC-DC converter", *IEEE Transactions on Circuits and Systems-1*, Vol.39, No.8, 1992, pp.680-683.
- [2] C.K.Tse, "Flip bifurcation and chaos in three-state boost switching regulators", *IEEE Transactions on Circuits and Systems-1*, Vol.41, No.1, 1994, pp. 16-23.
- [3] S.Banerjee, K.Chakrabarty, "Nonlinear modelling and bifurcation in the boost converter", *IEEE Transactions on Power Electronics*, Vol.13, No.2, 1998, pp. 252-260.
- [4] I.Zafrani, S.Ben-Yankov, "A chaos model of subharmonic oscillations in current mode PWM boost converters", *Proc.IEEE Power Electronic Special Conference PESC 95*, 1995.
- [5] D.Pelin, I.Flegar, "Chaotic behaviour of a boost converter", *Proc. XXIV International Convention MIPRO*, May 21 – 25, 2001, Opatija, Croatia.